Catalytic Properties of ADAM12 and Its Domain Deletion Mutants†

Jonas Jacobsen,*,‡,§ Robert Visse,§ Hans Peter Sørensen,‡ Jan J. Enghild,|| Keith Brew,⊥ Ulla M. Wewer,‡ and Hideaki Nagase§

Department of Biomedical Sciences and Biotech Research & Innovation Centre (BRIC), University of Copenhagen, Ole Maaløes Vej 5, DK-2200 Copenhagen, Denmark, Kennedy Institute of Rheumatology Division, Faculty of Medicine, Imperial College London, 1 Aspenlea Road, London W6 8LH, United Kingdom, Department of Molecular Biology, University of Aarhus, Science park, Gustav Wieds vej 10C, DK-8000 Aarhus C, Denmark, and Department of Biomedical Science, Florida Atlantic University, Boca Raton, Florida 33431

Received August 13, 2007; Revised Manuscript Received November 9, 2007

ABSTRACT: Human ADAM12 (a disintegrin and metalloproteinase) is a multidomain zinc metalloproteinase expressed at high levels during development and in human tumors. ADAM12 exists as two splice variants: a classical type 1 membrane-anchored form (ADAM12-L) and a secreted splice variant (ADAM12-S) consisting of pro, catalytic, disintegrin, cysteine-rich, and EGF domains. Here we present a novel activity of recombinant ADAM12-S and its domain deletion mutants on S-carboxymethylated transferrin (Cm-Tf). Cleavage of Cm-Tf occurred at multiple sites, and N-terminal sequencing showed that the enzyme exhibits restricted specificity but a consensus sequence could not be defined as its subsite requirements are promiscuous. Kinetic analysis revealed that the noncatalytic C-terminal domains are important regulators of Cm-Tf activity and that ADAM12-PC consisting of the pro domain and catalytic domain is the most active on this substrate. It was also observed that NaCl inhibits ADAM12. Among the tissue inhibitors of metalloproteinases (TIMP) examined, the N-terminal domain of TIMP-3 (N-TIMP-3) inhibits ADAM12-S and ADAM12-PC with low nanomolar $K_{i(app)}$ values while TIMP-2 inhibits them with a slightly lower affinity (9−44 nM). However, TIMP-1 is a much weaker inhibitor. N-TIMP-3 variants that lack MMP inhibitory activity but retained the ability to inhibit ADAM17/TACE failed to inhibit ADAM12. These results indicate unique enzymatic properties of ADAM12 among the members of the ADAM family of metalloproteinases.

A disintegrin and metalloproteinase ADAM12,[1] also known as meltrin α, is a multifunctional zinc-dependent enzyme that belongs to a subfamily of reprolysin metallopeptidases (*1*−*3*). Human ADAM12 is expressed as a classical type 1 membrane-anchored form (ADAM12-L) and as a secreted splice variant (ADAM12-S) (*1*). The latter consists of a propeptide, a catalytic domain, and cell adhesive disintegrin-, cysteine-rich-, and epidermal growth factor-like (EGF-like) domains (Figure 1A) but lacks the C-terminal transmembrane and cytoplasmic domains. Both forms are strongly expressed in placenta, and decreased serum levels of ADAM12 in pregnant women are reliable biomarkers for preeclampsia and Down's syndrome in clinical prenatal diagnostics (*1*, *4*−*7*). Low expression levels of ADAM12 are found in most normal adult tissues, but the level of expression is greatly increased in different types of cancers (*8*−*11*). In the polyoma middle T antigen (PymT) mouse model of breast cancer, ADAM12 stimulated tumor progression by increasing the tumor burden and decreasing the time to tumor onset (*12*). Importantly, ADAM12 is readily detected in urine of breast and bladder cancer patients and correlates with disease status and stage (*13*, *14*).

The three-dimensional structure of ADAM12 has not yet been determined experimentally. Using electron microscopy, we modeled the overall domain organization of ADAM12-S containing the pro domain as a compact four-leaf clover-like molecule (*15*). This model was supported by the recently determined structure of a snake venom homologue of mammalian ADAMs, vascular apoptosis inducing protein 1 (VAP1) (*16*) consisting of the catalytic domain, disintegrin, and cysteine-rich domains. Crystal structures for the catalytic domains of homologues tumor necrosis factor-α-converting enzyme (TACE or ADAM17) (*17*) and ADAM33 (*18*) have been determined. Both structures reveal a polypeptide fold consisting of a five-stranded β-sheet surrounded by five α-helices, resembling the folding of the catalytic domains of the related zinc metalloproteinases collectively called the metzincins (*19*).

On the basis of its zinc-binding consensus sequence motif *HEXXHXXGXXH*, ADAM12 was predicted to be an active

† U.M.W. was supported by the Danish Cancer Society, the Danish Medical Council, Novo Nordic, the Lundbeck Foundation, and the Munksholm Foundation, and H.N. was supported by NIH Grant AR 40994 and The Wellcome Trust Grant 07547.

* To whom correspondence should be addressed. Telephone: +45-35326081. Fax: +45-35325669. E-mail: jonas@pai.ku.dk.

‡ University of Copenhagen.

§ Imperial College London.

|| University of Aarhus.

⊥ Florida Atlantic University.

[1] Abbreviations: ADAM12, disintegrin and metalloprotease; EGF, epidermal growth factor; PymT, polyoma middle T antigen; VAP1, vascular apoptosis-inducing proteins; TACE, tumour necrosis factor-α-converting enzyme; α_2M, α2-macroglobulin; IGFBP, insulin-like growth factor binding protein; P-LAP, placental leucine aminopeptidase; HB-EGF, heparin binding EGF-like growth factor; TIMP, tissue inhibitor of metalloprotease; Cm-Tf, carboxymethylated transferrin.

10.1021/bi701629c CCC: $40.75 © 2008 American Chemical Society
Published on Web 12/15/2007

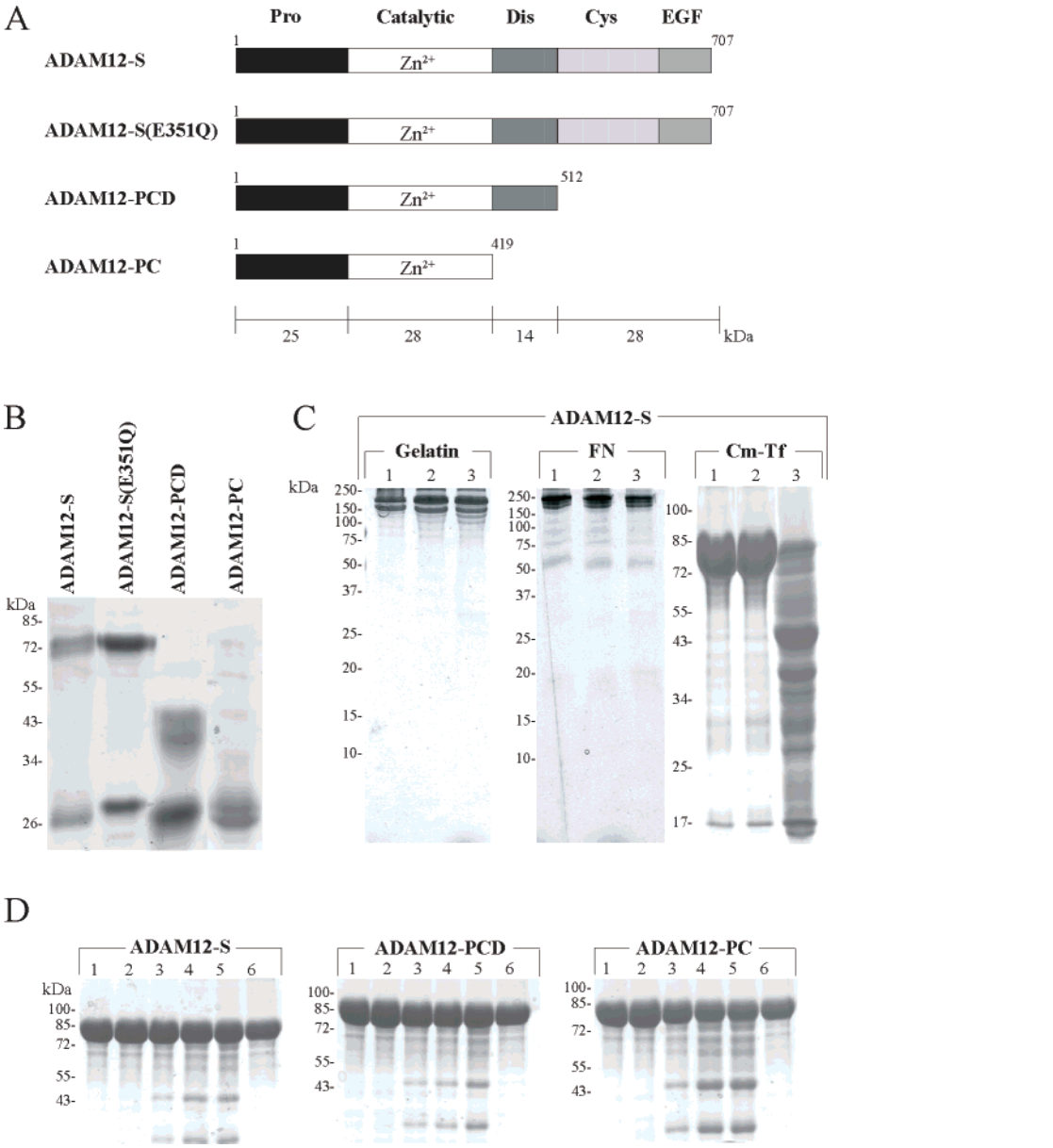

FIGURE 1: SDS−PAGE analysis of recombinant ADAM12 and detection of proteolytic activity. (A) Full-length ADAM12-S and its domain deletion mutants are shown with their experimentally determined molecular masses. Pro stands for the pro domain, Cat for the catalytic domain, Dis for the disintegrin domain, Cys for the cysteine-rich domain, and EGF for the EGF-like domain. (B) The purities of the recombinant proteins were analyzed by SDS−PAGE (12% acryl-amide), and the proteins were stained using Coomassie Brilliant Blue R-250. (C) The activity of ADAM12-S was assayed with gelatin, fibronectin, and Cm-Tf for 24 h in 50 mM Tris-HCl (pH 7.5), 0.05% Brij 35, and 0.02% sodium azide: lane 1, substrate at 0 h; lane 2, substrate after 24 h; and lane 3, incubation with 100 nM enzyme. (D) All three variants of ADAM12 were employed in a time course study of Cm-Tf degradation. Reaction buffer contained 0.5 mM $CaCl_2$: lane 1, substrate at 0 h; lane 2, substrate after 18 h; lane 3, enzyme for 1 h; lane 4, enzyme for 8 h; lane 5, enzyme for 18 h; and lane 6, enzyme and 20 mM EDTA for 18 h.

metzincin metalloproteinase, and its catalytic activity was originally verified using the α2-macroglobulin (α_2M) entrapment assay (*20*, *21*). Potential physiological substrates include insulin-like growth factor binding proteins IGFBP-3 and -5 (*4*, *22*), placental leucine aminopeptidase (P-LAP) (*23*), heparin binding EGF-like growth factor (HB-EGF) (*24*), EGF, and betacellulin (*25*). These substrates are also susceptible to other metalloproteases (reviewed in refs *3*, *26*, and *27*), and the relative contribution of ADAM12-mediated cleavage of these substrates in vivo is poorly understood. Previous studies have shown that ADAM12 latency can be explained by the cysteine switch mechanism in which Cys179 in the pro domain coordinates the active site zinc ion (*21*, *28*). The enzyme is processed in the trans-Golgi at the proprotein convertase recognition motif RHKR, and following translocation to the plasma membrane or extracellular space, ADAM12 is considered to be present in its active form (*21*, *28*). However, the pro domain remains noncovalently associated with the mature enzyme following cleavage (*15*, *22*), indicating possible extracellular functions of the pro domain. Our previous in vitro characterization of the catalytic activity of ADAM12 using α2M reactivity indicated that this activity requires Cu^{2+}, and we proposed that this activity was revealed through binding of the transition ion Cu^{2+} to the unpaired Cys273 (*29*). ADAM12 is inhibited by the tissue inhibitor of metalloproteinases 3 (TIMP-3) (*22*), and other inhibitors of ADAM12 include the synthetic hydroxymate inhibitors GM6001 and its derivative

KB-R7785 (*24*), TMI-1 (*30*), and a group of dipeptide analogues (*31*).

Although a number of biological molecules have been described as potential substrates of ADAM12, little is known about the biochemical properties of the catalytic activity of ADAM12. Nevertheless, the close association of ADAM12 with severe pathological disorders underlines the relevance of addressing the biochemical properties of ADAM12-mediated proteolysis. Here we present reduced S-carboxymethylated transferrin (Cm-Tf) (*32*) as a novel ADAM12 substrate suitable for kinetic studies. Using this substrate, we assessed the sequence specificity of ADAM12 and quantitatively compared the effect of salts, cations, and inhibitors on the activity of ADAM12-S and its truncated mutant consisting of the pro and catalytic domains. Our studies have demonstrated that ADAM12 is a protease with a slight alkaline preference, which is very sensitive to increases in ionic strength. Furthermore, our data suggest that the TIMP susceptibility of ADAM12 is significantly different from that of ADAM 17/TACE.

EXPERIMENTAL PROCEDURES

Materials. The pCEP-4 vector was from Invitrogen (Groningen, The Netherlands), and restriction enzymes were purchased from New England Biolabs (Hithin, U.K.). Human apotransferrin was from Sigma. Human fibronectin was purified from plasma according to the method of Ruoslahti and Engvall (*33*). Gelatin was formed by heating type 1 collagen purified from guinea pig skin at 65 °C for 20 min as described previously (*34*). Fluorescent peptide substrate [dabcyl-LAQAhomoPheRSK(5FAM)-NH_2] was from BioZyme, Inc.

Human recombinant TIMP-1 and TIMP-2 were expressed in mammalian cells and purified as described previously (*35*, *36*). The N-terminal domain of TIMP-1 (N-TIMP-1) was expressed and purified as described by Wei et al. (*37*). Expression in *Escherichia coli*, purification, and in vitro folding of N-TIMP-3 and the N-TIMP-3 mutant with an extra Ala added at the N-terminus [-1A]N-TIMP-3 as well as N-TIMP-3(T2G) have all been described previously (*38*, *39*).

Generation of Recombinant ADAM12 Proteins. cDNA encoding human ADAM12 (GenBank entry NM_021641) constructs in the pCEP4 plasmid were generated as previously reported (*15*). The constructs were (i) full-length ADAM12-S consisting of the pro domain, catalytic domain, disintegrin domain, cysteine-rich domain, and EGF-like domain (amino acids 1−707), (ii) ADAM12-PCD encoding the pro domain, catalytic domain, and disintegrin domain (amino acids 1−512), and (iii) ADAM12-PC encoding the pro domain and catalytic domain (amino acids 1−419). The ADAM12 signal peptide was present in all plasmids. The plasmid harboring the ADAM12-S full-length cDNA was used as a template for site-directed mutagenesis to generate the catalytic site E351Q mutant (amino acids 1−707). HEK 293 EBNA cells grown in DMEM containing 10% FBS, penicillin, and streptomycin were transfected with the desired construct using lipofectamine. Serum-free conditioned media were harvested, centrifuged, and filtered through a 0.22 μm filter prior to a triple FPLC purification procedure. First, the medium was subjected to gelatin−Sepharose chromatography. Next, the flow through containing the recombinant was passed through a SP-Sepharose-FF column where the protein was retained and subsequently eluted using a gradient of 0.05 to 1 M NaCl. The recombinant proteins were further purified by a concanavalin A column and elution with α-D-methyl mannopyranoside as described previously (*11*, *22*).

Proteolytic Assay of ADAM12. Human transferrin was S-carboxymethylated under reducing conditions with iodoacetic acid as described previously (*40*). After TCA precipitation, the Cm-Tf was dissolved in dH_2O and adjusted to pH 7.0−8.0 by titration with NaOH. Proteolysis assays were carried out in 12.5 mM Tris-HCl at pH 8.5 containing 0.5 mM $CaCl_2$, 0.02% NaN_3, and 0.05% Brij 35 unless otherwise stated. All reagents (5 μL of enzyme, 5 μL of buffer, and 10 μL of substrate) were mixed and briefly centrifuged prior to incubation at 37 °C for various periods of time. The reaction was stopped by addition of reducing SDS−PAGE sample buffer containing 20 mM EDTA, and the products were separated using SDS−PAGE (10% total acrylamide) and stained using Coomassie Brilliant Blue R-250. Enzyme concentrations varied between 1.5 and 25 nM, and the concentration of Cm-Tf was 70 μM. Detailed assay conditions for each experiment are specified in the figure legends. All data presented are the average of at least three representative experiments and include standard errors.

N-Terminal Sequencing of Cm-Tf Fragments. For N-terminal sequence analysis, Cm-Tf was digested with 750 nM ADAM12-S for 2 h, and cleaved products were separated using SDS−PAGE, electrotransferred to a polyvinylidene difluoride membranes, and visualized by Coomassie Brilliant Blue R-250 staining. Samples were analyzed by automated Edman degradation using an Applied Biosystems Procise 494HT sequencer with on-line phenylthiohydantoin HPLC analysis.

Densitometric Analysis. SDS−PAGE gels were scanned at 300 dpi using a flatbed scanner. The intensity of the selected 43 kDa degradation product was quantified using the TL100 software (Nonlinear Dynamics, Newcastle upon Tyne, U.K.).

K_m and k_{cat} Determination. For studies of steady-state kinetics, the molar concentration of Cm-Tf was calculated from A_{280} observations ($\epsilon = 85\,240$), and a fixed concentration of enzyme was incubated with Cm-Tf dilutions between 3.75 and 70 μM prepared in dH_2O. Activity was plotted against substrate concentration, and K_m could be obtained when points were fitted to the Michaelis−Menten rate equation [$V = V_{max}[S]/(K_m + [S])$] using GraphPad Prism. k_{cat} was calculated as the number of molecules of Cm-Tf consumed per second per active site of enzyme. For this purpose, the active site concentrations of ADAM12-S, ADAM12-PCD, and ADAM12-PC were determined by titration with α_2M. The pixel volume of the 43 kDa cleavage product was converted to weight units by comparison with known amounts of bovine serum albumin loaded on the same Tris-glycine gel.

Determination of pH-Dependent Activity. To maintain a constant ionic strength across the tested pH range (pH 6.0−9.0), we utilized the acetate/2-(*N*-morpholino)ethanesulfonic acid (MES)/Tris (AMT) buffer system (*41*). The pH was adjusted with NaOH or HCl, and the final concentrations in the assay were as follows: 12.5 mM sodium acetate, 25 mM Tris-HCl, 12.5 mM MES, 0.5 mM $CaCl_2$, 0.02% sodium azide, and 0.05% Brij 35.

Studies of ADAM12 Inhibition Kinetics. The concentrations of TIMP-1, N-TIMP-1, TIMP-2, and N-TIMP-3 inhibitors were determined by active site titration with a known concentration of MMP-1, and N-TIMP-3(2TG), N-TIMP-3, and [-1A]N-TIMP-3 were titrated with a known concentration of ADAMTS-5. Various concentrations of TIMPs were mixed with 2 nM ADAM12-S or 1.5 nM ADAM12-PC in 25 mM Tris-HCl (pH 8.0), 1.25 mM $CaCl_2$, and 18.75 mM NaCl in a total volume of 15 μL and incubated for 30 min at 37 °C. The mixture was then incubated with 5 μL of Cm-Tf (140 μM) at 37 °C for 9 h. Studies with N-TIMP-3 and N-TIMP-3 mutants included 2.5% glycerol to prevent precipitation. The reaction was stopped with reducing sample buffer containing 20 mM EDTA. The products were separated using SDS−PAGE (10% total acrylamide) and stained using Coomassie Brilliant Blue R-250. IC_{50} values were determined by linear regression analysis of residual activity plotted against log values of inhibitor concentration. For tight binding inhibitors at low enzyme concentrations (at $\sim K_i$), this represents a good approximation of the $K_{i(app)}$ (*42*).

The K_i values of N-TIMP-3 against ADAM12-S and ADAM12-PC were obtained using the fluorescent substrate [dabcyl-LAQAhomoPheRSK(5FAM)-NH_2] and the Morrison equation describing tight binding inhibition (*30*, *43*). Buffer conditions were identical to those of inhibitor studies using Cm-Tf as a substrate, though 5% DMSO was included to increase the solubility of the substrate; 85 μL of assay buffer, 5 μL of inhibitor, and 5 μL of enzyme (2 nM, final concentration) were preincubated at 37 °C for 2 h prior to the addition of 5 μL of substrate (10 μM, final concentration). A BMG Fluorostar Optima fluorometer (excitation at 485 nm and emission at 530 nm) was used to monitor fluorescence.

RESULTS

Purification and Detection of ADAM12-S and Its Domain Deletion Mutants. Full-length ADAM12-S and its C-terminally truncated domain deletion mutants as well as the ADAM12-S(E351Q) mutant (Figure 1A) were expressed in HEK 293 EBNA cells and purified from the conditioned media. The recombinant enzyme preparations were free from visible contaminants as determined by SDS−polyacrylamide gel electrophoresis and staining with Coomassie Brilliant Blue R-250 (Figure 1B). Also, they reacted with ADAM12 domain specific antisera (data not shown). ADAM12-PCD shows a double band around 45 kDa. Both bands react with antisera directed against the catalytic domain (data not shown), suggesting possible processing of the C-terminus (*15*). The experimentally determined sizes are bigger than the theoretical M_r calculated from the amino acid composition. This can possibly be explained by predicted N-linked glycosylations at two sites in the pro domain, and one site in all other domains except the EGF-like domain. The presence of the copurified but noncovalently linked ~26 kDa propeptide has previously been observed (*15*, *22*) and is confirmed here.

Catalytic Activity of ADAM12 and Its Domain Deletion Mutants. The catalytic properties of purified ADAM12-S were first evaluated using three different substrates. Each substrate was incubated with 100 nM ADAM12-S in 50 mM Tris-HCl (pH 7.5) for 24 h at 37 °C and subjected to SDS−PAGE analysis, essentially as described by Roy et al. (*13*). As seen in Figure 1C, degradation of gelatin and fibronectin (FN) was not observed. However, when samples were assayed using the general protease substrate carboxymethylated transferrin (Cm-Tf), several degradation products were observed (Figure 1C). Not only wild-type ADAM12-S but also the domain deletion mutants ADAM12-PCD and ADAM12-PC were shown to cleave Cm-Tf (Figure 1D). Cm-Tf cleavage patterns generated by the three isoforms of ADAM12 were identical, indicating that the lack of ancillary C-terminal domains does not affect substrate specificity on Cm-Tf (data not shown). Even at a concentration of 1 μM and after incubation for 48 h, the catalytic site mutant ADAM12-S(E351Q) did not degrade the substrate, confirming the importance of the glutamic acid in catalysis and indicating that the purified enzymes were free of contaminating proteases (data not shown). All ADAM12 isoforms were inhibited by 20 mM EDTA (Figure 1D, lanes 6) and by TIMP-2 and the N-terminal domain of TIMP-3 (N-TIMP-3) (see Table 2).

Table 1: Substrate Affinities and Turnover Numbers[a]

	K_m	k_{cat}	k_{cat}/K_m
ADAM12-S	14.5 ± 1.6	0.12 ± 0.01	8.3×10^3
ADAM12-PCD	19.2 ± 1.2	0.18 ± 0.02	9.4×10^3
ADAM12-PC	16.5 ± 1.3	0.47 ± 0.06	28.4×10^3

[a] K_m, in micromolar, and k_{cat}, in inverse seconds, were determined from three replications as described in Experimental Procedures.

N-Terminal Sequencing of Cm-Tf Cleavage Products. The degradation of Cm-Tf with ADAM12-S yielded several products (Figure 2A). The restricted number of products suggests that ADAM12 does not cleave Cm-Tf randomly. To analyze the sequence required for ADAM12 activity, we conducted N-terminal sequence analysis of Cm-Tf degradation products. A total of 15 bands were sequenced, and eight of these contained more than one sequence in which the recovery of phenylthiohydantoin amino acids was of comparable concentration. VPDKTV sequences represent the mature N-termini of full-length transferrin and are therefore not informative. On the basis of their size and rapid appearance, the two degradation products of 43 and 37 kDa (Figure 2A) are likely to represent the initial hydrolysis of full-length Cm-Tf into N- and C-terminal fragments. All other Cm-Tf degradation bands appear later in time course studies (data not shown). The identified amino acid residues with P1′ positions were Ala, Leu, Met, Val, Tyr, Ser, Asp, and Cm-Cys (Figure 2A,B). Cm-Cys (resembling glutamic acid) was detected only once in the P1′ position and three times in the P1 position. Aligning the cleavage sequences from P18 to P18′ did not reveal any clear consensus sequence requirement for ADAM12 cleavage (Figure 2B). To give further insight into the sequence requirement of ADAM12, the homologous N- and C-terminal domains of Cm-Tf were aligned and the sequence sites subsequently compared (Figure 2C), but once again, no common message could be extracted.

Enzyme Kinetics Using the Cm-Tf Substrate. To quantify enzymatic activity against Cm-Tf, we first carried out experiments to determine the time and dose dependency of ADAM12-S, ADAM12-PCD, and ADAM12-PC degradation of Cm-Tf. The digested samples were subjected to SDS−

Table 2: Apparent Inhibition Constants [$K_{i(app)}$] of ADAM12 Inhibitors[a]

	ADAM12-S	ADAM12-PC	MMP-3(ΔC)[b]	TACE[b]
TIMP-1	454 ± 161	110 ± 2		
N-TIMP-1	400 ± 98	506 ± 103		
TIMP-2	44 ± 16	9.3 ± 2.5		
N-TIMP-3	K_i = 12.5 ± 1.1[c]	K_i = 3.2 ± 0.25[c]	67 ± 2.8	13.7 ± 0.2
[-1A]N-TIMP-3	629 ± 147	816 ± 81	~3.3×10^3	33.9 ± 2.8
N-TIMP-3(T2G)	194 ± 48	307 ± 22	>1×10^4	35.6 ± 1.9

[a] Values were obtained from the average of three replications, calculated as described in Experimental Procedures and given in nanomolar. [b] Data obtained from ref *37*. [c] Due to limitations of the Cm-Tf assay, the $K_{i(app)}$ values of N-TIMP-3 inhibition could not be determined reliably. Instead, we used a fluorescent peptide substrate to determine substrate-independent K_i values.

PAGE, stained with Coomassie Brilliant Blue R-250, and analyzed by densitometry (data not shown). We selected a 43 kDa cleavage product for quantification, and the pixel volumes were taken as a measure of activity. This band was selected because it appeared rapidly and separated fairly well from surrounding degradation products. From these studies, it was evident that the formation of the Cm-Tf 43 kDa degradation product was linear up to 80 000 pixels, corresponding to a substrate turnover of less than 10% (data not shown). As the substrate appeared to be homogeneous and consist mainly of full-length Cm-Tf, the K_m of the substrate with the enzyme was determined by incubating a fixed concentration of enzyme with increasing amounts of substrate, which resulted in the classical hyperbolic-shaped curve (data not shown). Nonlinear regression using the Michaelis−Menten equation revealed that ADAM12-S, ADAM12-PCD, and ADAM12-PC had comparable K_m values of 14.5 ± 1.6, 19.2 ± 1.2, and 16.5 ± 1.3 μM, respectively (Table 1). Interestingly, calculation of the substrate specificity, k_{cat}/K_m, of the three isoforms (Table 1) showed a 4-fold increase in the ratio in the absence of the noncatalytic disintegrin and cysteine-rich domains, primarily due to an increase in k_{cat} values (Table 1).

pH Optimum of ADAM12-S and ADAM12-PC. An evaluation of the effect of pH on enzymatic activity was carried out with the Cm-Tf substrate using the AMT triple buffer system to ensure a constant ionic strength over the entire pH range that was tested. Both ADAM12-S and ADAM12-PC exhibited optimal activities at a slightly alkaline pH of 8.0−8.5 (Figure 3). The enzyme activity could not be detected at pH values lower than 6.5, and ~50% enzyme activity was detected at pH values of 7.5 and 9.

Calcium Requirement and Salt Sensitivity of ADAM12-S and ADAM12-PC. When the sequence of the ADAM12 catalytic domain is examined in relation to the crystal structure of the catalytic domains of ADAM33, VAP1, and VAP2B, it strongly suggests the presence of a single fully conserved structurally important Ca^{2+} coordination site opposing the active site cleft (*16*, *18*, *44*). In fact, many metalloproteinases such as MMPs (*45*) and ADAMTS-13 (*46*) require calcium for activity. We found that ADAM12-S was active when placed in a calcium-free buffer (Figure 4A). The activity was increased by only ~50% upon addition of 250−500 μM $CaCl_2$, while higher concentrations were less effective. An apo-ADAM12-S generated by EDTA treatment followed by dialysis showed no activity and required calcium in addition to zinc for reactivation (data not shown). Furthermore, we found that NaCl had an inhibitory effect on ADAM12-S with an IC_{50} value of 31 ± 3 mM, and even addition of 500 μM $CaCl_2$ was not able to produce any significant recovery of activity (Figure 4B). ADAM12-PC was also active in the calcium-depleted buffer, and a profile of the salt inhibitory effect comparable to that of ADAM12-S was obtained (Figure 4C). The estimated IC_{50} value of NaCl inhibition of ADAM12-PC was 49 ± 6 mM. The high sensitivity of both ADAM12-S and ADAM12-PC to increased ionic strength was also seen with potassium ions or Tris-HCl (data not shown).

Effect of Other Metal Ions on ADAM12-S Activity. In a previous qualitative study of ADAM12 proteolysis, Cu^{2+} was implicated in the activation of ADAM12 (*29*). We decided to reassess this quantitatively to determine the requirement of ADAM12 catalytic activity for biologically relevant metal ions. Addition of $ZnCl_2$ at concentrations below 50 μM increased the activity of ADAM12-S by approximately 30%. However, when concentrations exceeded 50 μM, activity was negatively affected, and at a concentration of 500 μM $ZnCl_2$, substrate degradation was only just detectable (Figure 5A). Besides Ca^{2+} and Zn^{2+}, only Mg^{2+} had a marginal stimulatory effect, while none of the other tested divalent cations were capable of inducing activity (Figure 5B). In contrast to an earlier report that used α_2M as a substrate (*29*), Cu^{2+} was not an activator of ADAM12-S. Rather, data suggested that even low levels of $CuCl_2$ had a negative effect on the ADAM12-S-mediated hydrolysis of Cm-Tf. Hg^{2+} and Mn^{2+} inhibited activity, whereas Fe^{2+} had practically no effect. Notably, 10 μM $CoCl_2$ inhibited the activity by 80%, while increasing concentrations rescued the lost activity. Low concentrations of $NiCl_2$ inhibited ADAM12-S drastically. The hydrolysis of Cm-Tf was inhibited by more than 50% in the presence of 1 μM $NiCl_2$ and was essentially absent at concentrations above 10 μM. Similar results were obtained for $NiCl_2$ in the presence of Ca^{2+} (Figure 5C). This suggests that the Ni^{2+} binding site is unrelated to the Ca^{2+} binding site.

Inhibition of ADAM12 by TIMPs. The catalytic activities of MMPs, ADAMTSs, and ADAMs are believed to be regulated by endogenous TIMPs in vivo. To determine the contributions of different TIMPs to ADAM12 regulation, we conducted studies of the inhibition of ADAM12-S and ADAM12-PC by wild-type and mutant TIMPs. The calculated K_i values are summarized in Table 2. TIMP-1 inhibited ADAM12-S with a $K_{i(app)}$ of 454 ± 161 nM but exhibited a 5-fold higher affinity toward the ADAM12-PC mutant. TIMP-2 was a more effective inhibitor of ADAM12, and some differences were observed between ADAM12-S and ADAM12-PC with the $K_{i(app)}$ values of 44 ± 16 and 9.3 ± 2.5 nM, respectively. To test if the differences in $K_{i(app)}$ values between ADAM12-S and ADAM12-PC were related to interactions between the C-terminal domains of enzyme and

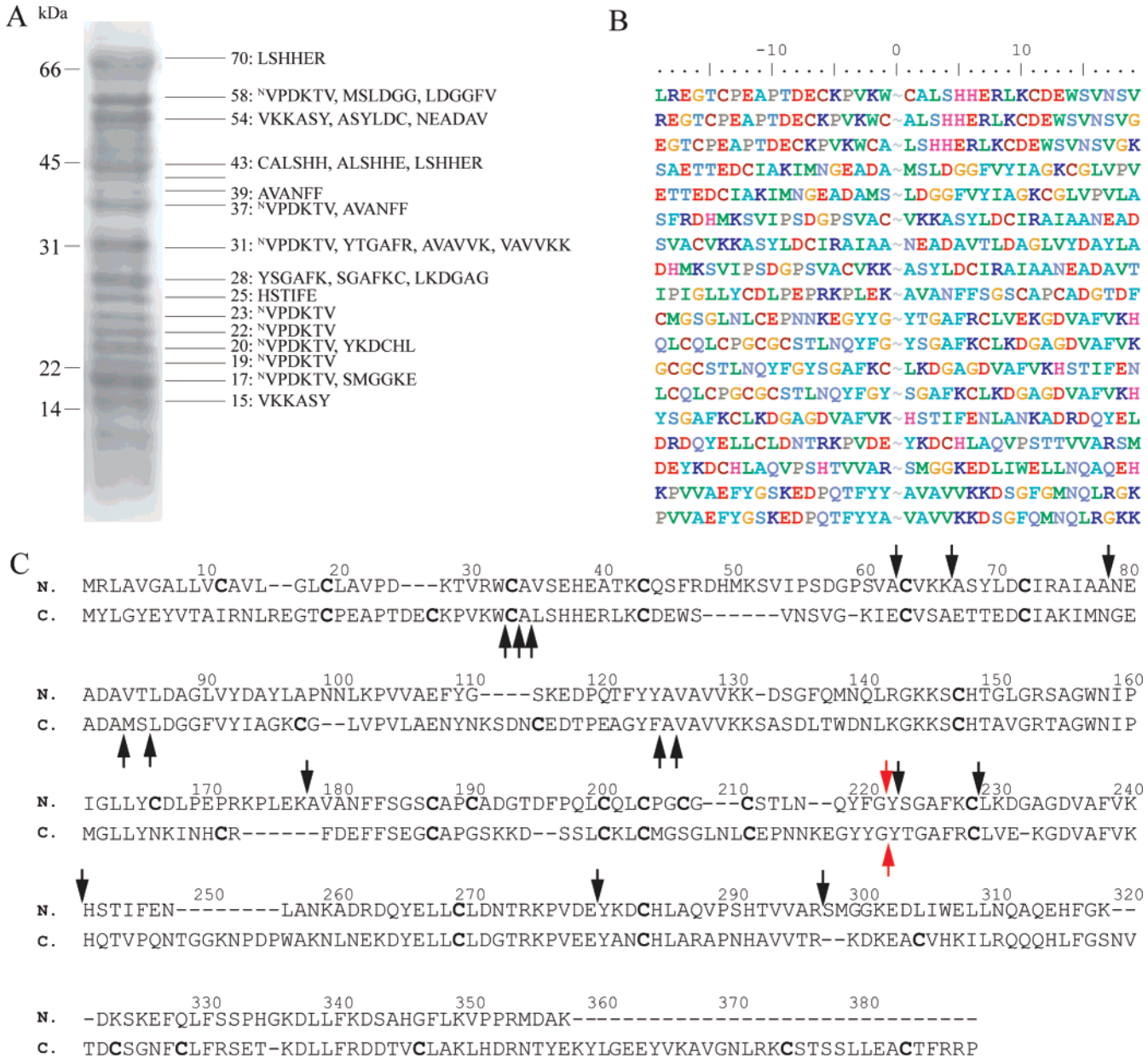

FIGURE 2: ADAM12-S cleavage sites in Cm-Tf. (A) Full-length Cm-Tf was digested with 750 nM ADAM12-S for 2 h. N-Terminal Edman degradation yielded sequences from 15 bands represented by their apparent molecular masses in kilodaltons. Sequences preceded with a superscript N refer to the N-terminus of full-length human transferrin. (B) The obtained sequences, 18 in total when N-terminal full-length Cm-Tf was excluded, were aligned using *Clustal W* and are color-coded. (C) The homologous N- and C-terminal domains were aligned using *Clustal W*, and cleavage sites are marked by arrows. Red arrows highlight the presence of a cleavage "pair". N-Terminal numbering of amino acids was included, and Cm-Cys is highlighted in bold.

inhibitor, an N-TIMP-1 variant was included in the study. When assayed under identical conditions, N-TIMP-1 turned out to have a lower affinity for ADAM12-PC with a $K_{i(app)}$ value of 506 ± 103 nM. The inadequate sensitivity of the Cm-Tf substrate did not allow for the correct determination of K_i values for the potent inhibition of N-TIMP-3 toward ADAM12. Since the ability of TIMP-3 to inhibit ADAM12 potently indicates that TIMP-3 is the physiological inhibitor of ADAM12, we thought it was important to determine the exact K_i value of this interaction. To do so, we utilized a fluorescent TNF-α-derived fluorescent peptide substrate recently reported to be ADAM12 sensitive (*30*). Under buffer conditions identical to those used in the Cm-Tf assay, substrate-independent K_i values of 12.5 ± 1.1 nM for ADAM12-S and 3.2 ± 0.25 nM for ADAM12-PC were obtained.

We then evaluated the inhibitory potency of N-TIMP-3 reactive site mutants which lack inhibitory activity for MMPs but retained activity against ADAM17 (*39*). These include [-1A]N-TIMP-3 which has an extra Ala at the N-terminus of N-TIMP-3 and N-TIMP-3(T2G) where Thr2 of TIMP-3 is mutated to Gly. In contrast to ADAM17, these two mutants were poor inhibitors for ADAM12-S and ADAM12-PC (Table 2). N-TIMP-3(T2G) inhibited ADAM12-S with a $K_{i(app)}$ value of 194 ± 48 nM and exhibited an even lower affinity for ADAM12-PC [$K_{i(app)}$ = 307 ± 22 nM], whereas [-1A]N-TIMP-3 was an even less effective inhibitor of the two ADAM12 isoforms.

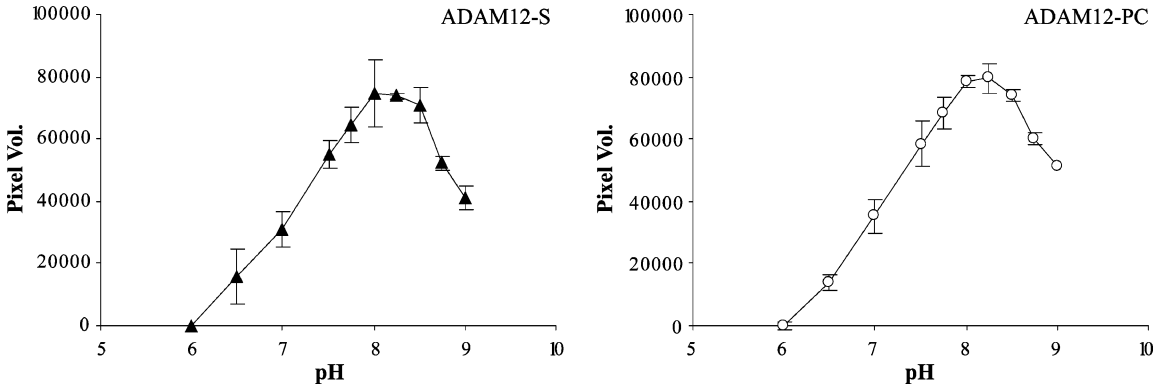

FIGURE 3: Dependency of ADAM12-S and ADAM12-PC activity on pH. The influence of pH on cleavage of Cm-Tf by ADAM12-S and ADAM12-PC was tested in the AMT buffer system. Besides the AMT buffer components, the reaction mixture contained 0.5 mM $CaCl_2$. Samples were incubated with 5 nM ADAM12-S (▲) or ADAM12-PC (○) for 3 or 2 h, respectively.

DISCUSSION

This paper reports the catalytic properties of recombinant human ADAM12-S and its domain deletion mutants ADAM12-PCD and ADAM12-PC. We first assessed the activity of ADAM12-S toward a number of potential substrates. Gelatin and fibronectin were both reported to be cleaved by ADAM12 (*13*), but our initial screen did not exhibit any detectable activities against these substrates. When redetermined under conditions optimized for ADAM12-S activity (pH 8.5 and 0.5 mM $CaCl_2$), activity was not detected against gelatin or fibronectin (data not shown). The discrepancy may be due to some contamination of other proteainases in those enzyme preparations as it was reported that EDTA failed to inhibit those activities (*13*). On the other hand, the three isoenzymes readily digested Cm-Tf (Figure 1C), a substrate used to detect activity of MMPs (*40*) and some ADAMTSs (*32*, *47*). The presence of contaminating proteases was excluded on the basis of TIMP-3 inhibition of the three enzymes and the inability of the ADAM12-S (E351Q) to cleave Cm-Tf.

Substrate Specificity. Even though ADAM12 has been reported to cleave IGFBP-3, IGFBP-5, HB-EGF, and a number of other substrates, its substrate specificity with regard to sequences cleaved has not been investigated. We have presented here the first data on the cleavage specificity of ADAM12. With regard to the S1′ specificity pocket, ADAM12 does not have a preference for specific amino acids and can accept residues with widely different physicochemical properties, including Ala, Leu, Met, Val, Tyr, Ser, Asp, and Cm-Cys. When the sequences of all 18 identified cleavage sites are aligned, it becomes evident that no strict consensus sequence can be recognized that is required for ADAM12 cleavage (Figure 2B). A similar promiscuity was reported for ADAMTS-4 (*32*) and ADAMTS-5 (*47*). The closest relatives of ADAM12, ADAM19, and ADAM33 were both reported to cleave an Ala−Leu bond in an insulin β-chain-derived peptide (*48*), and ADAM19 has been found to cleave between Lys and Ala in myelin basic protein (*49*). We observed that ADAM12 was capable of cleaving similar bonds in Cm-Tf (Figure 2). An advantage of using Cm-Tf degradation for investigation of sequence specificity is that the C-terminal and N-terminal halves of human transferrin are homologous (Figure 2C) (*50*). Examination of the enzyme cleavage sites in a sequence alignment of the N- and C-terminal domains of Cm-Tf can provide useful information about the effects of amino acid substitutions around the cleavage site. One example of a cleavage "pair" in the N-terminal and C-terminal domains deduced from sites in the present study is the G−Y bond highlighted with red arrows in Figure 2C. Unfortunately, the residues around these two cleavage sites are similar, and therefore, this analysis does not give much insight into the specificity. The presence of juxtaposed cleavage sites, e.g., such as the ones seen in the 43 kDa band and the 28 kDa fragments, might suggest that exosite binding or secondary structures of the substrate are key determinants, while some degrees of freedom are allowed at the cleavage site as originally suggested by Kashiwagi et al. (*32*). Since clustered cleavage sites can be found only in a limited number of places and the residues cleaved are promiscuous, we propose that ADAM12 functions only as an endopeptidase rather than an endo- and exopeptidase to cleave the clustered sites.

For comparison, the pregnancy-associated plasma protein-A (PAPP-A)-mediated cleavage of IGFBP-4 is highly dependent on conserved basic residues located up to 16 amino acids N-terminal of the scissile bond (*51*). Another similar example is the inability of ADAMTS aggrecanases to cleave peptides shorter than 30 amino acids (*52*). Once the physiological substrate of ADAM12 has been determined, it will be of great interest to establish the biologically relevant cleavage site.

Catalytic Properties. Removal of C-terminal disintegrin, cysteine-rich, and EGF domains had little or no effect on the K_m, suggesting that the affinity for substrate is unchanged (Table 1); however, at the same time, the k_{cat} for Cm-Tf cleavage was increased. ADAM12-PC was approximately 4-fold more active, while ADAM-PCD exhibited a 1.5-fold increase in activity. This indicates that the cysteine-rich and, in particular, the disintegrin domain reduce the activity of the enzyme possibly by affecting the environment of the catalytic site or inducing conformational changes. These results may be partially contrasted by ADAMTS-4 where the full-length enzyme has little activity on Cm-Tf, but when the C-terminal spacer domain is deleted, it exhibits activity with Cm-Tf whereas the catalytic domain alone has little activity (*32*).

To extend our knowledge of ADAM12 proteolysis, we characterized the cleavage of Cm-Tf with regard to the salt dependency, pH, and effects of metal cations. Sequence alignment revealed that the catalytic domain of ADAM12

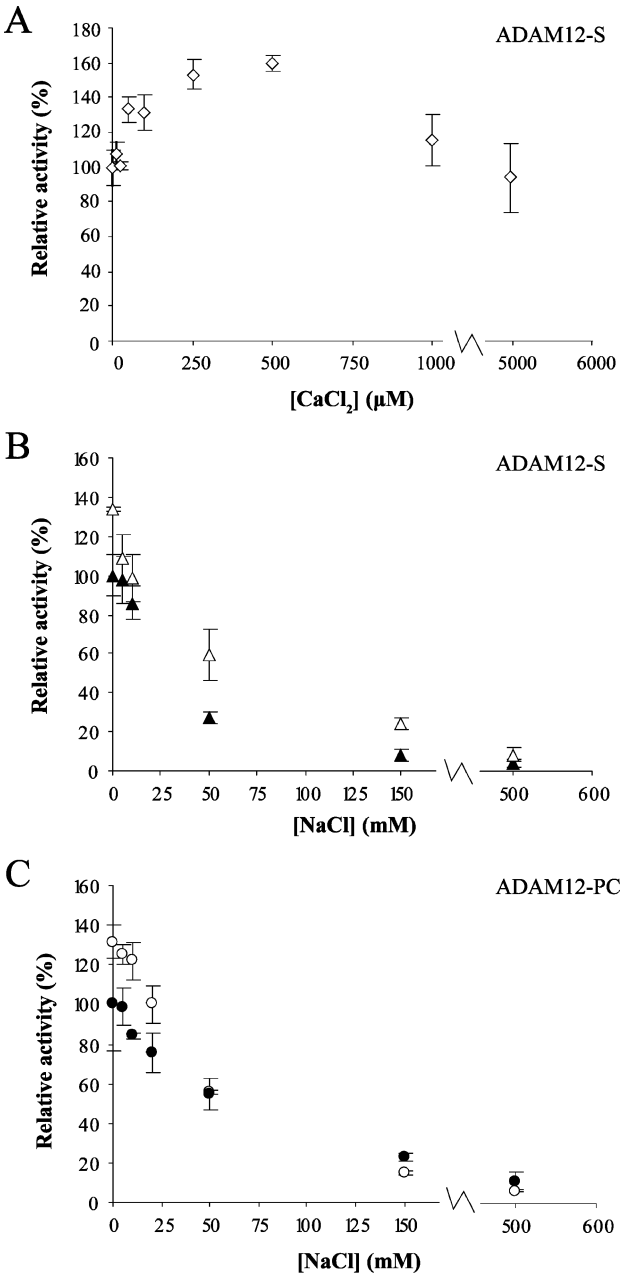

FIGURE 4: Influence of $CaCl_2$ and NaCl on the enzymatic activity of ADAM12-S and ADAM12-PC. (A) $CaCl_2$- and NaCl-free solutions of enzymes were prepared by dialysis against a buffer containing 25 mM Tris-HCl (pH 8.5), 0.05% Brij 35, and 0.02% sodium azide. Then, $CaCl_2$ (0−5 mM) was titrated into an ADAM12-S (◇) assay, and activity was expressed as a percentage of the control activity measured under $CaCl_2$- and NaCl-depleted conditions. (B) Under identical conditions, the inhibitory effect of NaCl was investigated for ADAM12-S in the absence (▲) and presence (△) of 0.5 mM $CaCl_2$. (C) Similarly, the influence of NaCl on ADAM12-PC in the absence (●) and presence (○) of 0.5 mM $CaCl_2$ was determined. Samples were incubated with 5 nM ADAM12-S or ADAM12-PC for 3 or 2 h, respectively.

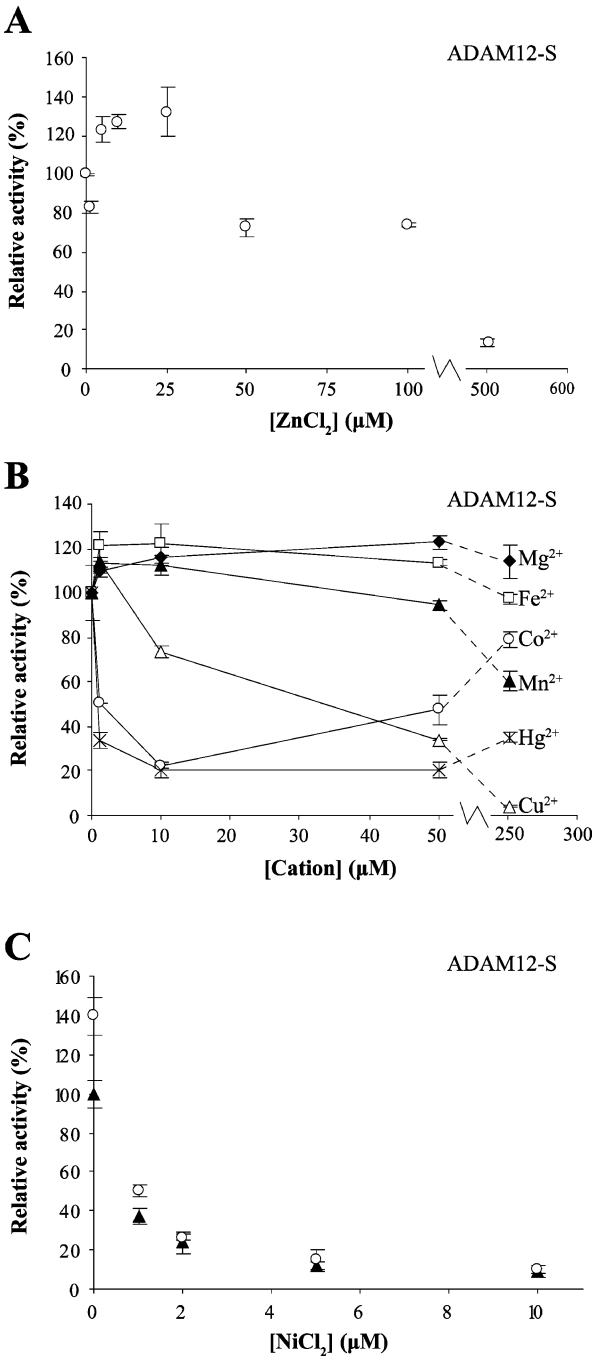

FIGURE 5: Dependency of ADAM12-S on metal ions in the absence of Ca^{2+}. (A) To determine the influence of Zn^{2+} on ADAM12-S cleavage of Cm-Tf, increasing concentrations of $ZnCl_2$ (0−0.5 mM) were added to an ADAM12-S (○) assay. (B) Six different divalent cations, Mg^{2+} (◆), Fe^{2+} (□), Co^{2+} (○), Mn^{2+} (▲), Hg^{2+} (×), and Cu^{2+} (△), were in a similar manner added (0−0.25 mM) to an ADAM12-S activity assay. For both panels A and B, activity was expressed as a percentage of the control activity measured in the absence of externally added cations. (C) Activity of ADAM12-S was assessed in the presence of $NiCl_2$ (0−10 μM) with (○) or without (▲) 0.5 mM $CaCl_2$ in the buffer, and activity was expressed in the same manner described above. All samples were incubated with 5 nM ADAM12-S for 3 h.

contains an acidic calcium binding consensus motif (*44*) known from other proteases to be essential for the structural integrity of their catalytic domains (*18*, *26*, *53*). Furthermore, in a recent publication on the crystal structure of vascular apoptosis-inducing protein-1 (VAP1), a snake venom homologue of ADAMs, it was shown that the disintegrin domain comprises two additional structural calcium binding sites that are fully conserved in ADAM12 (*16*). ADAM12-S and ADAM12-PC were active on Cm-Tf in a calcium-free buffer, and an optimal concentration of 0.5 mM $CaCl_2$ increased ADAM12-S activity by ~50% (Figure 4A). Apo-ADAM12-S was on the other hand not active without the addition of both calcium and zinc to the buffer verifying the importance of calcium. Since we observed a similar fold

increase in activity upon the addition of $CaCl_2$ to either ADAM12-S or ADAM12-PC, we believe that calcium at least binds the catalytic domain. In comparison, the activity of other metalloproteases, e.g., ADAMTS-13 (*46*) and MMP-3 (*45*), is much more dependent upon the addition of Ca^{2+} to the assay to yield optimal activity.

The sensitivity to increases in ionic strength displayed by ADAM12 is intriguing (Figure 4B,C). Similar salt sensitivity has been observed for other metalloproteinases, including ADAM17 (*54*), PAPP-A (*51*), ADAMTS-13 (*55*), and mitochondrial processing peptidase (MPP) (*51*, *54*−*56*). Electrostatic interactions between charged surfaces on the enzyme and the substrate are known to be greatly important for substrate recognition in MPP and TACE (*54*, *57*). Theoretically, this can be projected onto ADAM12 where electrostatic surface potential modeling predicted the surface area surrounding the catalytic cleft of ADAM12 to be mainly negatively charged (*44*). If electrostatic interactions with the substrate are important in ADAM12, then certain cleavage sites in Cm-Tf could theoretically be favored over others when the ionic strength is increased. However, there was no difference in the Cm-Tf cleavage patterns in the presence and absence of physiological NaCl concentrations (data not shown). Alternatively, increased hydrophobicity in the presence of high salt may result in inappropriate interaction of the substrate with subsites in the substrate binding site, thus reducing the enzymatic activity.

The active site of ADAM12 is considered to contain a catalytic Zn^{2+} ion which when coordinated by a polarized water molecule assists in a nucleophilic attack of the carbonyl carbon of the scissile bond of the substrate. When $ZnCl_2$ was added to the assay, we observed a small increase in activity of approximately 30% at 25 μM, and at higher concentrations, hydrolysis was adversely affected (Figure 5A). This inhibitory effect can potentially be explained by the formation of harmful $Zn(OH)^+$ that binds to glutamate in the active site (*58*). The activities of other metalloproteinases, such as MMP-1 and MMP-3, that share metal ion binding properties with ADAM12 are affected by other divalent cations besides Ca^{2+} and Zn^{2+} (*59*−*61*). Only Mg^{2+} enhanced ADAM12-S activity, whereas Ni^{2+}, Hg^{2+}, and Cu^{2+} potently inhibited the enzyme activity (Figure 5B,C). These cation inhibition profiles closely resemble those of astacin (*62*). Crystal structures of astacin complexed with Ni^{2+} and Hg^{2+} showed less availability in terms of the water molecule essential for catalysis. Similar steric changes may potentially explain the diminished proteolytic activity that we observed for ADAM12. In contrast to an earlier report on Cu^{2+} activation of ADAM12 measured by α_2M entrapment (*29*), our experiments show that ADAM12-S is negatively affected by $CuCl_2$. Cu^{2+} may exhibit an opposing effect on the activity of ADAM12 depending on the substrate. The dual role of $CoCl_2$ as both an inhibitor and an activator of ADAM12-S and the inhibitory effect of $NiCl_2$ ($IC_{50} < 1$ μM) are interesting, but they cannot be readily explained.

The activity of ADAM12-S and ADAM12-PC is abrogated below pH 6.5 (Figure 3). This may be in part due to protonation of the histidines ($pK_a \sim 6.5-7$), thereby affecting the coordination of the active site zinc ion. Activity peaks in the pH 8−8.5 range and several other zinc peptidases have shown a similar preference for a slightly alkaline environment (*51*, *53*).

ProADAM12 is processed at the furin cleavage site, presumably in the trans-Golgi (*28*). Following cleavage, the pro domain remains noncovalently associated with the mature enzyme, yet the enzyme expresses proteolytic activity (*29*). It is not known how the pro domain contributes to this activity as we have not yet been able to successfully obtain the catalytic domain without the pro domain. The recombinant form fails to be expressed without the pro domain in mammalian cells (our observations and ref *21*). A clear understanding of the function of the pro domain in the catalytic activity of ADAM12 requires the resolution of the three-dimensional structure of ADAM12.

TIMP Inhibition of ADAM12. It is generally thought that the inhibitory activity of TIMP-1 and TIMP-2 is restricted to MMPs with a few exceptions such as the TIMP-1 inhibition of ADAM-10 (*63*). We found full-length TIMP-2 to be a potent inhibitor of both ADAM12-S and ADAM12-PC (Table 1). To the best of our knowledge, this is the first study to show potent inhibition of a member of the ADAM family by TIMP-2. The study also showed that N-TIMP-3 is the strongest inhibitor of both ADAM12-PC and ADAM12-S. The K_i values of 12.5 ± 1.1 nM for the inhibition of ADAM12-S and 3.2 ± 0.25 nM for the inhibition of ADAM12-PC obtained using the fluorescent substrate indicated that TIMP-3 is the physiological inhibitor of ADAM12, perhaps together with TIMP-2. Overall, the tested TIMPs seem to have a higher affinity for the truncated ADAM12-PC than for full-length ADAM12-S. These results indicate that the C-terminal domains in ADAM12-S weaken the inhibitory action of TIMPs as seen for TACE previously (*64*).

Recently, Wei et al. (*39*) reported that the substitution of Thr for Gly2 [N-TIMP-3(T2G)] or the addition of an N-terminal Ala extension ([-1A]N-TIMP-3) abrogated MMP inhibition, but their inhibitory activity toward ADAM17 (TACE) was not affected significantly (*39*). We therefore tested these two mutants for their abilities to inhibit ADAM12 and found that both failed to inhibit ADAM12 potently. This observation is noteworthy, since it resembles what was seen for the MMPs but not for the more closely related ADAM17/TACE (*39*).

One major challenge in the treatment of pathological disorders such as arthritis and cancer with protease inhibitors is nonspecific inhibition. In this light, it is encouraging to see that the broad-range metalloprotease inhibitor TIMP-3 can be designed to discriminate not only between ADAMs and MMPs but also within the ADAM family itself. This observation is encouraging for the future design of specific TIMP-derived inhibitors suitable for treatment of pathological disorders caused by altered metalloproteinase activities. It will be important to extend these studies to different TIMP-sensitive subfamilies of the metzincins such as the ADAMs and ADAMTSs.

ACKNOWLEDGMENT

We thank Ida B. Tøgersen for conducting N-terminal sequence analysis.

REFERENCES

1. Gilpin, B. J., Loechel, F., Mattei, M. G., Engvall, E., Albrechtsen, R., and Wewer, U. M. (1998) A novel, secreted form of human ADAM 12 (meltrin α) provokes myogenesis in vivo, *J. Biol. Chem. 273*, 157−166.

2. Yagami-Hiromasa, T., Sato, T., Kurisaki, T., Kamijo, K., Nabeshima, Y., and Fujisawa-Sehara, A. (1995) A metalloprotease-disintegrin participating in myoblast fusion, *Nature 377*, 652−656.
3. Seals, D. F., and Courtneidge, S. A. (2003) The ADAMs family of metalloproteases: Multidomain proteins with multiple functions, *Genes Dev. 17*, 7−30.
4. Shi, Z. D., Xu, W. Z., Loechel, F., Wewer, U. M., and Murphy, L. J. (2000) ADAM 12, a disintegrin metalloprotease, interacts with insulin-like growth factor-binding protein-3, *J. Biol. Chem. 275*, 18574−18580.
5. Laigaard, J., Sorensen, T., Frohlich, C., Pedersen, B. N., Christiansen, M., Schiott, K., Uldbjerg, N., Albrechtsen, R., Clausen, H. V., Ottesen, B., and Wewer, U. M. (2003) ADAM12: A novel first-trimester maternal serum marker for Down syndrome, *Prenatal Diagn. 23*, 1086−1091.
6. Laigaard, J., Sorensen, T., Placing, S., Holck, P., Frohlich, C., Wojdemann, K. R., Sundberg, K., Shalmi, A. C., Tabor, A., Norgaard-Pedersen, B., Ottesen, B., Christiansen, M., and Wewer, U. M. (2005) Reduction of the disintegrin and metalloprotease ADAM12 in preeclampsia, *Obstet. Gynecol. 106*, 144−149.
7. Laigaard, J., Christiansen, M., Frohlich, C., Pedersen, B. N., Ottesen, B., and Wewer, U. M. (2005) The level of ADAM12-S in maternal serum is an early first-trimester marker of fetal trisomy 18, *Prenatal Diagn. 25*, 45−46.
8. Iba, K., Albrechtsen, R., Gilpin, B. J., Loechel, F., and Wewer, U. M. (1999) Cysteine-rich domain of human ADAM 12 (meltrin α) supports tumor cell adhesion, *Am. J. Pathol. 154*, 1489−1501.
9. Kodama, T., Ikeda, E., Okada, A., Ohtsuka, T., Shimoda, M., Shiomi, T., Yoshida, K., Nakada, M., Ohuchi, E., and Okada, Y. (2004) ADAM12 is selectively overexpressed in human glioblastomas and is associated with glioblastoma cell proliferation and shedding of heparin-binding epidermal growth factor, *Am. J. Pathol. 165*, 1743−1753.
10. Kveiborg, M., Frohlich, C., Albrechtsen, R., Tischler, V., Dietrich, N., Holck, P., Kronqvist, P., Rank, F., Mercurio, A. M., and Wewer, U. M. (2005) A role for ADAM12 in breast tumor progression and stromal cell apoptosis, *Cancer Res. 65*, 4754−4761.
11. Thodeti, C. K., Frohlich, C., Nielsen, C. K., Holck, P., Sundberg, C., Kveiborg, M., Mahalingam, Y., Albrechtsen, R., Couchman, J. R., and Wewer, U. M. (2005) Hierarchy of ADAM12 binding to integrins in tumor cells, *Exp. Cell Res. 309*, 438−450.
12. Kveiborg, M., Frohlich, C., Albrechtsen, R., Tischler, V., Dietrich, N., Holck, P., Kronqvist, P., Rank, F., Mercurio, A. M., and Wewer, U. M. (2005) A role for ADAM12 in breast tumor progression and stromal cell apoptosis, *Cancer Res. 65*, 4754−4761.
13. Roy, R., Wewer, U. M., Zurakowski, D., Pories, S. E., and Moses, M. A. (2004) ADAM 12 cleaves extracellular matrix proteins and correlates with cancer status and stage, *J. Biol. Chem. 279*, 51323−51330.
14. Frohlich, C., Albrechtsen, R., Dyrskjot, L., Rudkjaer, L., Orntoft, T. F., and Wewer, U. M. (2006) Molecular profiling of ADAM12 in human bladder cancer, *Clin. Cancer Res. 12*, 7359−7368.
15. Wewer, U. M., Morgelin, M., Holck, P., Jacobsen, J., Lydolph, M. C., Johnsen, A. H., Kveiborg, M., and Albrechtsen, R. (2006) ADAM12 is a four-leafed clover: The excised prodomain remains bound to the mature enzyme, *J. Biol. Chem. 281*, 9418−9422.
16. Takeda, S., Igarashi, T., Mori, H., and Araki, S. (2006) Crystal structures of VAP1 reveal ADAMs' MDC domain architecture and its unique C-shaped scaffold, *EMBO J. 25*, 2388−2396.
17. Maskos, K., Fernandez-Catalan, C., Huber, R., Bourenkov, G. P., Bartunik, H., Ellestad, G. A., Reddy, P., Wolfson, M. F., Rauch, C. T., Castner, B. J., Davis, R., Clarke, H. R. G., Petersen, M., Fitzner, J. N., Cerretti, D. P., March, C. J., Paxton, R. J., Black, R. A., and Bode, W. (1998) Crystal structure of the catalytic domain of human tumor necrosis factor-α-converting enzyme, *Proc. Natl. Acad. Sci. U.S.A. 95*, 3408−3412.
18. Orth, P., Reichert, P., Wang, W. Y., Prosise, W. W., Yarosh-Tomaine, T., Hammond, G., Ingram, R. N., Xiao, L., Mirza, U. A., Zou, J., Strickland, C., Taremi, S. S., Le, H. V., and Madison, V. (2004) Crystal structure of the catalytic domain of human ADAM33, *J. Mol. Biol. 335*, 129−137.
19. Gomis-Ruth, F. X. (2003) Structural aspects of the metzincin clan of metalloendopeptidases, *Mol. Biotechnol. 24*, 157−202.
20. Loechel, F., Gilpin, B. J., Engvall, E., Albrechtsen, R., and Wewer, U. M. (1998) Human ADAM 12 (meltrin α) is an active metalloprotease, *J. Biol. Chem. 273*, 16993−16997.
21. Loechel, F., Overgaard, M. T., Oxvig, C., Albrechtsen, R., and Wewer, U. M. (1999) Regulation of human ADAM 12 protease by the prodomain: Evidence for a functional, cysteine switch, *J. Biol. Chem. 274*, 13427−13433.
22. Loechel, F., Fox, J. W., Murphy, G., Albrechtsen, R., and Wewer, U. M. (2000) ADAM 12-S cleaves IGFBP-3 and IGFBP-5 and is inhibited by TIMP-3, *Biochem. Biophys. Res. Commun. 278*, 511−515.
23. Ito, N., Nomura, S., Iwase, A., Ito, T., Kikkawa, F., Tsujimoto, M., Ishiura, S., and Mizutani, S. (2004) ADAMs, a disintegrin and metalloproteinases, mediate shedding of oxytocinase, *Biochem. Biophys. Res. Commun. 314*, 1008−1013.
24. Asakura, M., Kitakaze, M., Takashima, S., Liao, Y., Ishikura, F., Yoshinaka, T., Ohmoto, H., Node, K., Yoshino, K., Ishiguro, H., Asanuma, H., Sanada, S., Matsumura, Y., Takeda, H., Beppu, S., Tada, M., Hori, M., and Higashiyama, S. (2002) Cardiac hypertrophy is inhibited by antagonism of ADAM12 processing of HB-EGF: Metalloproteinase inhibitors as a new therapy, *Nat. Med. 8*, 35−40.
25. Horiuchi, K., Le Gall, S., Schulte, M., Yamaguchi, T., Reiss, K., Murphy, G., Toyama, Y., Hartmann, D., Saftig, P., and Blobel, C. P. (2007) Substrate selectivity of epidermal growth factor-receptor ligand sheddases and their regulation by phorbol esters and calcium influx, *Mol. Biol. Cell 18*, 176−188.
26. Nagase, H., Visse, R., and Murphy, G. (2006) Structure and function of matrix metalloproteinases and TIMPs, *Cardiovasc. Res. 69*, 562−573.
27. Becherer, J. D., and Blobel, C. P. (2003) Biochemical properties and functions of membrane-anchored metalloprotease-disintegrin proteins (ADAMs), *Curr. Top. Dev. Biol. 54*, 101−123.
28. Cao, Y., Kang, Q., Zhao, Z. F., and Zolkiewska, A. (2002) Intracellular processing of metalloprotease disintegrin ADAM12, *J. Biol. Chem. 277*, 26403−26411.
29. Loechel, F., and Wewer, U. M. (2001) Activation of ADAM 12 protease by copper, *FEBS Lett. 506*, 65−68.
30. Moss, M. L., and Rasmussen, F. H. (2007) Fluorescent substrates for the proteinases ADAM17, ADAM10, ADAM8, and ADAM12 useful for high-throughput inhibitor screening, *Anal. Biochem. 366*, 144−148.
31. Oh, M., Im, I., Lee, Y. J., Kim, Y. H., Yoon, J. H., Park, H. G., Higashiyama, S., Kim, Y. C., and Park, W. J. (2004) Structure-based virtual screening and biological evaluation of potent and selective ADAM12 inhibitors, *Bioorg. Med. Chem. Lett. 14*, 6071−6074.
32. Kashiwagi, M., Enghild, J. J., Gendron, C., Hughes, C., Caterson, B., Itoh, Y., and Nagase, H. (2004) Altered proteolytic activities of ADAMTS-4 expressed by C-terminal processing, *J. Biol. Chem. 279*, 10109−10119.
33. Engvall, E., and Ruoslahti, E. (1978) Immunochemical and collagen-binding properties of fibronectin, *Ann. N.Y. Acad. Sci. 312*, 178−191.
34. Itoh, Y., Binner, S., and Nagase, H. (1995) Steps Involved in Activation of the Complex of Pro-Matrix Metalloproteinase-2 (Progelatinase-A) and Tissue Inhibitor of Metalloproteinases (Timp)-2 by 4-Aminophenylmercuric Acetate, *Biochem. J. 308*, 645−651.
35. Huang, W., Suzuki, K., Nagase, H., Arumugam, S., VanDoren, S. R., and Brew, K. (1996) Folding and characterization of the amino-terminal domain of human tissue inhibitor of metalloproteinases-1 (TIMP-1) expressed at high yield in *E. coli*, *FEBS Lett. 384*, 155−161.
36. Troeberg, L., Tanaka, M., Wait, R., Shi, Y. E., Brew, K., and Nagase, H. (2002) *E. coli* expression of TIMP-4 and comparative kinetic studies with TIMP-1 and TIMP-2: Insights into the interactions of TIMPs and matrix metalloproteinase 2 (gelatinase A), *Biochemistry 41*, 15025−15035.
37. Wei, S., Chen, Y., Chung, L., Nagase, H., and Brew, K. (2003) Protein engineering of the tissue inhibitor of metalloproteinase 1 (TIMP-1) inhibitory domain: In search of selective matrix metalloproteinase inhibitors, *J. Biol. Chem. 278*, 9831−9834.
38. Kashiwagi, M., Tortorella, M., Nagase, H., and Brew, K. (2001) TIMP-3 is a potent inhibitor of aggrecanase 1 (ADAM-TS4) and aggrecanase 2 (ADAM-TS5), *J. Biol. Chem. 276*, 12501−12504.
39. Wei, S., Kashiwagi, M., Kota, S., Xie, Z. H., Nagase, H., and Brew, K. (2005) Reactive site mutations in tissue inhibitor of metalloproteinase-3 disrupt inhibition of matrix metalloproteinases but not tumor necrosis factor-α-converting enzyme, *J. Biol. Chem. 280*, 32877−32882.

40. Nagase, H. (1995) Human stromelysins 1 and 2, *Methods Enzymol. 248*, 449−470.
41. Ellis, K. J., and Morrison, J. F. (1982) Buffers of Constant Ionic Strength for Studying pH-Dependent Processes, *Methods Enzymol. 87*, 405−426.
42. Bieth, J. G. (1995) Theoretical and practical aspects of proteinase inhibition kinetics, *Methods Enzymol 248*, 59−84.
43. Williams, J. W., and Morrison, J. F. (1979) The kinetics of reversible tight-binding inhibition, *Methods Enzymol. 63*, 437−467.
44. Andreini, C., Banci, L., Bertini, I., Elmi, S., and Rosato, A. (2005) Comparative analysis of the ADAM and ADAMTS families, *J. Proteome Res. 4*, 881−888.
45. Housley, T. J., Baumann, A. P., Braun, I. D., Davis, G., Seperack, P. K., and Wilhelm, S. M. (1993) Recombinant Chinese-Hamster Ovary Cell Matrix Metalloprotease-3 (Mmp-3, Stromelysin-1): Role of Calcium in Promatrix Metalloprotease-3 (Pro-Mmp-3, Prostromelysin-1) Activation and Thermostability of the Low Mass Catalytic Domain of Mmp-3, *J. Biol. Chem. 268*, 4481−4487.
46. Anderson, P. J., Kokame, K., and Sadler, J. E. (2006) Zinc and Calcium Ions Cooperatively Modulate ADAMTS13 Activity, *J. Biol. Chem. 281*, 850−857.
47. Gendron, C., Kashiwagi, M., Lim, N. H., Enghild, J. J., Thogersen, I. B., Hughes, C., Caterson, B., and Nagase, H. (2007) Proteolytic activities of human ADAMTS-5: Comparative studies with human ADAMTS-4, *J. Biol. Chem.* (in press).
48. Zou, J., Zhu, F., Liu, J. J., Wang, W. Y., Zhang, R. M., Garlisi, C. G., Liu, Y. H., Wang, S. H., Shah, H., Wan, Y. T., and Umland, S. P. (2004) Catalytic activity of human ADAM33, *J. Biol. Chem. 279*, 9818−9830.
49. Chesneau, V., Becherer, J. D., Zheng, Y. F., Erdjument-Bromage, H., Tempst, P., and Blobel, C. P. (2003) Catalytic properties of ADAM19, *J. Biol. Chem. 278*, 22331−22340.
50. Macgillivray, R. T. A., Mendez, E., Sinha, S. K., Sutton, M. R., Linebackzins, J., and Brew, K. (1982) The Complete Amino-Acid-Sequence of Human-Serum Transferrin, *Proc. Natl. Acad. Sci. U.S.A. 79*, 2504−2508.
51. Laursen, L. S., Overgaard, M. T., Nielsen, C. G., Boldt, H. B., Hopmann, K. H., Conover, C. A., Sottrup-Jensen, L., Giudice, L. C., and Oxvig, C. (2002) Substrate specificity of the metalloproteinase pregnancy-associated plasma protein-A (PAPP-A) assessed by mutagenesis and analysis of synthetic peptides: Substrate residues distant from the scissile bond are critical for proteolysis, *Biochem. J. 367*, 31−40.
52. Miller, J. A., Liu, R. Q., Davis, G. L., Pratta, M. A., Trzaskos, J. M., and Copeland, R. A. (2003) A microplate assay specific for the enzyme aggrecanase, *Anal. Biochem. 314*, 260−265.
53. Furlan, M., Robles, R., and Lammle, B. (1996) Partial purification and characterization of a protease from human plasma cleaving von Willebrand factor to fragments produced by in vivo proteolysis, *Blood 87*, 4223−4234.
54. Milla, M. E., Leesnitzer, M. A., Moss, M. L., Clay, W. C., Carter, H. L., Miller, A. B., Su, J. L., Lambert, M. H., Willard, D. H., Sheeley, D. M., Kost, T. A., Burkhart, W., Moyer, M., Blackburn, R. K., Pahel, G. L., Mitchell, J. L., Hoffman, C. R., and Becherer, J. D. (1999) Specific sequence elements are required for the expression of functional tumor necrosis factor-α-converting enzyme (TACE), *J. Biol. Chem. 274*, 30563−30570.
55. Majerus, E. M., Anderson, P. J., and Sadler, J. E. (2004) Characterization of the binding interaction between ADAMTS13 and von Willebrand factor (VWF), *Blood 104*, 150A.
56. Kitada, S., and Ito, A. (2001) Electrostatic recognition of matrix targeting signal by mitochondrial processing peptidase, *J. Biochem. 129*, 155−161.
57. Taylor, A. B., Smith, B. S., Kitada, S., Kojima, K., Miyaura, H., Otwinowski, Z., Ito, A., and Deisenhofer, J. (2001) Crystal structures of mitochondrial processing peptidase reveal the mode for specific cleavage of import signal sequences, *Structure 9*, 615−625.
58. Auld, D. S. (1995) *Methods Enzymol. 248*, 228−242.
59. Salowe, S. P., Marcy, A. I., Cuca, G. C., Smith, C. K., Kopka, I. E., Hagmann, W. K., and Hermes, J. D. (1992) Characterization of Zinc-Binding Sites in Human Stromelysin-1: Stoichiometry of the Catalytic Domain and Identification of a Cysteine Ligand in the Proenzyme, *Biochemistry 31*, 4535−4540.
60. Hojima, Y., Behta, B., Romanic, A. M., and Prockop, D. J. (1994) Cadmium Ions Inhibit Procollagen C-Proteinase and Cupric Ions Inhibit Procollagen N-Proteinase, *Matrix Biol. 14*, 113−120.
61. Okada, Y., Nagase, H., and Harris, E. D. (1986) A Metalloproteinase from Human Rheumatoid Synovial Fibroblasts That Digests Connective-Tissue Matrix Components: Purification and Characterization, *J. Biol. Chem. 261*, 4245−4255.
62. Gomisruth, F. X., Grams, F., Yiallouros, I., Nar, H., Kusthardt, U., Zwilling, R., Bode, W., and Stocker, W. (1994) Crystal Structures, Spectroscopic Features, and Catalytic Properties of Cobalt(II), Copper(II), Nickel(II), and Mercury(II) Derivatives of the Zinc Endopeptidase Astacin: A Correlation of Structure and Proteolytic Activity, *J. Biol. Chem. 269*, 17111−17117.
63. Amour, A., Knight, C. G., Webster, A., Slocombe, P. M., Stephens, P. E., Knauper, V., Docherty, A. J. P., and Murphy, G. (2000) The in vitro activity of ADAM-10 is inhibited by TIMP-1 and TIMP-3, *FEBS Lett. 473*, 275−279.
64. Lee, M. H., Verma, V., Maskos, K., Becherer, J. D., Knauper, V., Dodds, P., Amour, A., and Murphy, G. (2002) The C-terminal domains of TACE weaken the inhibitory action of N-TIMP-3, *FEBS Lett. 520*, 102−106.

BI701629C